Emergence of Filamentary Structure in Cosmological Gravitational Clustering

B.S. Sathyaprakash and Varun Sahni

Inter-University Centre for Astronomy & Astrophysics, Post Bag 4, Ganeshkhind, Pune 411007, India

Sergei F . Shandarin

Department of Physics and Astronomy, University of Kansas, Lawrence, KS 66045

ABSTRACT

The morphological nature of structures that form under gravitational instability has been of central interest to cosmology for over two decades. A remarkable feature of large scale structures in the Universe is that they occupy a relatively small fraction of the volume and yet show coherence on scales comparable to the survey size. With the aid of a useful synthesis of percolation analysis and shape statistics we explore the evolution of morphology of isolated density clumps in *real space* and that of the cluster [1] distribution as a whole in scale-invariant cosmological models of gravitational instability. Our results, based on an exhaustive statistical analysis, indicate that at finite density thresholds one-dimensional filaments are more abundant than two-dimensional sheets (pancakes) at most epochs and for all spectra although the first singularities could be pancakelike. Both filamentarity and pancakeness of structures grow with time (in scale-free models this is equivalent to an increase in resolution) leading to the development of a long coherence length scale in simulations.

---

[1] In this paper we call a cluster any connected region with density above a given threshold.

Visually structures on scales of $\sim$ 50-100 Mpc can readily be discerned in the distribution of galaxies, in fact virtually all available catalog's reveal structures of the same size as the scale of the survey. A related and not completely understood issue concerns the morphology of structures (such as the Great Wall) observed both in the Universe and in our numerical simulations of it. Over a decade ago, and long before large galaxy catalogs were available, Zel'dovich (1982) wondered at the smallness of the filling factor of the galaxy distribution and Shandarin (1983) suggested the use of percolation theory to explore the topological properties of the distribution of galaxies (see brief summary in Shandarin & Zel'dovich (1983)). Owing partly to the peculiar shapes of galaxy survey volumes and partly to our lack of understanding as to how to apply percolation analysis under such circumstances, there has till very recently not been much progress in this direction. (For a recent study of percolation analysis of LSS see eg. Klypin & Shandarin (1993), Dominik & Shandarin (1992), Yess & Shandarin (1996) and Sathyaprakash, Sahni & Shandarin (1995). For a review of other discriminators of large scale structure see Sahni & Coles (1995).) Although, percolation properties alone are not very useful in quantifying the morphology of structure they do aid in its qualitative understanding as illustrated by the following argument: the *percolation transition* in an infinite volume characterizes the transition from a state in which no "infinite" cluster exists to one with an infinite cluster. For a random Poisson distribution of points it is well known that the percolation transition occurs at a filling factor of 0.319 (in three dimensions).

One way of understanding this is to imagine that each particle in a distribution is surrounded by a 'sphere of influence' of radius R. We can hop from one particle to the next if the inter-particle separation is smaller than $2R$. Clearly if R is too small traversing the entire length of the box in this manner is impossible. By increasing R however, a critical value R_c is reached at which percolation occurs and it becomes possible to travel across the entire box by jumping from one particle to the next. In the case of a Poisson random distribution of points the fraction of volume occupied by the union of equal spheres centered around every particle is about 32% of the total volume at the percolation threshold. Visually a random process does not possess any distinctive features, consequently the infinite cluster is expected to occupy a sizable fraction of the total volume in clusters as indeed it does. However, particles that are initially distributed randomly do acquire visually recognizable features while evolving under gravitational instability, additionally the percolation transition occurs at significantly lower filling factors at late times. In fact the percolating phase occupies a fraction of the total volume as small as 2-7% in models such as CDM and CHDM (Klypin & Shandarin 1993). This immediately suggests that individual structures within the percolating phase are unlikely to be spherical but ought to be more like sheets or filaments. In fact lower filling factors at the percolation transition are likely to

favor structures that are filamentary rather than planar (*i.e.* one-dimensional rather than two-dimensional), since the former occupy a comparatively smaller volume than the latter.

In order to quantify morphology we have to resort to statistical indicators other than percolation. In recent years several such measures have been introduced. After a careful study (Sathyaprakash et al. 1995a) we have chosen the structure functions of Babul and Starkman (1992) to characterize morphology of structure at the percolation transition. In our opinion these structure functions are quite robust and unbiased and are consistent with the visual impression that one forms from a given simulation. In the remainder of this Letter we describe the percolation properties and the evolution of morphology of *the mass distribution in real space* in scale-invariant models evolving under gravitational instability. A detailed report of our study will be published elsewhere (Sathyaprakash et al. 1995a).

The models we have studied are N-body simulations of scale invariant spectra with power spectrum $P(k) \equiv \left\langle |\delta_k|^2 \right\rangle \propto k^n$, for $k < k_{Ny}$, and $P(k) = 0$ for $k \geq k_{Ny}$, $n = -3, -2$, -1 0 and $+1$, where k_{Ny} is the Nyquist cutoff, δ_k is the Fourier transform of the density contrast $\delta(\mathbf{x}) = (\rho(\mathbf{x}) - \overline{\rho})/\overline{\rho}$, $\rho(\mathbf{x})$ being the density and $\overline{\rho}$ its average, $\langle \; \rangle$ denotes the average over an ensemble. We consider several epochs σ each characterized by the scale of nonlinearity k_{NL}^{-1} at that epoch determined by

$$\sigma \equiv \left\langle \delta^2 \right\rangle^{1/2} = D_+(t) \left(4\pi \int_0^{k_{\mathrm{NL}}} P(k) k^2 dk \right)^{1/2} = 1 \tag{1}$$

where $D_+(t)$ is the linear growing-mode solution of density fluctuations. N-body simulations are performed on a grid of size 128^3 using an equivalent number of particles and employing a particle-mesh algorithm (for details see Melott & Shandarin 1993). At each epoch density fields are constructed on a reduced grid of size 64^3 using a cloud-in-cell (CIC) algorithm [2] and our studies of percolation and morphology are carried out on these fields. For the sake of brevity we present results only for $n = -2$ and $n = 0$ models, at epochs when the nonlinear length scale is one of the following: $k_{\mathrm{NL}} = 64$, 16 and 4 in Fig. 1 & 2; $k_{\mathrm{NL}} = 32$, 16, 8 and 4 in Fig. 3; k_{NL} is measured in units of the fundamental mode $k_f \equiv 2\pi/L$, L being the length of the simulation box. Results obtained for other models are qualitatively similar to those reported here and will be discussed elsewhere [Sathyaprakash et al. 1995a].

Percolation theory, among other things, aims at studying the behavior of the volume of the largest cluster as a function of the density threshold or equivalently the filling factor

---

[2] We use a simple CIC algorithm in which the mass in a particle is reassigned to its six nearest neighbor lattice points: if the distance to a lattice point from the particle is (x, y, z) then the mass assigned of the former is $(1-x)(1-y)(1-z)$. Smearing, such as the one we employ, amounts to smoothing the density field by removing fluctuations on the Nyquist frequency scale.

(FF). At a given density threshold δ a cluster is identified as a connected overdense region, connectivity being defined using nearest neighbors. In Fig. 1 we have shown the results of percolation analysis of density fields obtained for the models described above; the scale of nonlinearity increases from top to bottom. The ratio of the fraction of volume in the largest cluster to the fraction of volume in all clusters (i.e. FF), denoted v_∞, is shown plotted against FF (thick solid line). The ratio of the total volume of all but the largest cluster to FF of overdense regions, denoted v_0, is also shown (thick dashed line). Error bars represent the dispersion in v_∞ and v_0 computed with the aid of four different realizations of a given spectrum of fluctuations. The thin vertical line in each panel corresponds to the *critical $FF = FF_c$* (or $\delta = \delta_c$) at which the percolation transition formally sets in (i.e. the opposite faces of the cube are linked); the region to the right of the line corresponds to the phase in which the largest cluster percolates and the region to the left corresponds to the phase in which it does not. It is clearly seen that FF_c is smaller (and the associated density threshold higher) for the $n = -2$ model relative to the $n = 0$ model. This may be related to the fact that the $n = -2$ model, has considerable large scale power making percolation easier in this case. With the onset of nonlinearity on larger scales (i.e. during later epochs) FF_c monotonically decreases for both models indicating the increasing coherence of structure as larger scales go nonlinear. The dispersion in the curves being small the features mentioned above are statistically significant. Thus we find that percolation analysis provides a sensitive probe of the nature of gravitational collapse in different scenarios of clustering (see also Yess & Shandarin 1996).

At a value slightly lower than FF_c the volume in all clusters except the largest one reaches a maximum (Yess & Shandarin 1996). This maximum is generic and occurs just before criticality irrespective of the spectrum of fluctuations and the stage of nonlinearity. At $FF > FF_c$ many small clusters link up with the largest cluster thereby aiding percolation, on the other hand at $FF < FF_c$, clusters tend to be sparse and gradually disappear as $FF \to 0$. Both these trends imply that the cluster distribution should peak before criticality which it does. We speculate that in an infinite, continuous system the occurrence of this maximum will coincide with FF_c; however the size and resolution of the present simulations are insufficient to unambiguously settle this issue which will be taken up in a future work. Thus, the percolation transition provides an objective choice of threshold at which to identify clusters. The results presented in this Letter concerning the morphology of structure are obtained by studying overdense regions slightly *below* the critical threshold in terms of the filling factor: $\sim FF_c$ (*above* the critical threshold in terms of the density contrast: $\delta > \delta_c$).

Babul and Starkman (1992) characterize the morphology of structure in a region of radius R around a given point using a triad of numbers which they call *structure functions.*

They begin with the first and second moments of the distribution of particles around a fiducial point. With the aid of these moments they construct the moment of inertia tensor and its associated eigenvalues. They then invoke a nonlinear transformation to arrive at three structure functions S_1, S_2 and S_3 each of which takes on values in the range [0,1] and exhibits unbiased behavior as a spherical distribution is continuously deformed either into a sheet or a filament, and a sheet is deformed into a filament (and vice-versa) (see [Babul & Starkman 1992, Sathyaprakash et al. 1995a] for more details). The triad of structure functions is given by

$$S_1 \equiv \sin\left[\frac{\pi}{2}(1-\mu)^p\right] \tag{2}$$

$$S_2 \equiv \sin\left[\frac{\pi}{2}a(\mu,\nu)\right] \tag{3}$$

$$S_3 \equiv \sin\left[\frac{\pi\nu}{2}\right] \tag{4}$$

where $\mu \equiv \sqrt{\lambda_2/\lambda_1}$, $\nu \equiv \sqrt{\lambda_3/\lambda_1}$ (λ_1, λ_2, and λ_3 being the three eigenvalues of the moment of inertia tensor arranged in decreasing order), the function $a(\mu,\nu)$ is implicitly defined by the equation

$$\frac{\mu^2}{a^2} - \frac{\nu^2}{a^2\left(1-\alpha a^{1/3}+\beta a^{2/3}\right)} = 1. \tag{5}$$

The values of parameters $p = \log 3/\log 1.5$, $\alpha = 1.9$ and $\beta = -(7/8)\ 9^{1/3} + \alpha\ 3^{1/3}$, are so chosen to normalize S_n. It is both instructive and legitimate to visualize the triad of structure functions as a vector $\mathbf{S} = (S_1, S_2, S_3)$ lying in the first octant of the three-dimensional space with magnitude $|\mathbf{S}| \leq 1$, the x-axis (say) characterizing linearity (filamentarity) S_1, the y-axis corresponding to planarity (oblateness) S_2, and the z-axis representing sphericity S_3, of the distribution of particles/points around a fiducial point. A vector lying along one of the x-, y- or z-axis is of unit magnitude by construction and represents, respectively, a perfectly linear, planar or spherically symmetric distribution of particles around the point in question. We shall however consider density fields defined on a grid, and *not* point processes, and use appropriately modified density weighted moments of the distribution. Such a modification overcomes the need to have particle positions and enhances the scope of the shape statistics as it can now be applied to study morphology of scalar fields in a variety of different contexts. (The quantity defined on the grid could be as diverse as: the surface brightness of a galaxy, the temperature of the sky as measured by a microwave background experiment, etc. It could also be a binary state taking on values 0/1.)

Conventionally the behavior of shape statistics has been studied as a function of the size of the region by averaging structure functions over a large ensemble of randomly chosen points (for an alternate application involving Minimal Spanning trees see [Pearson & Coles

1995]). In addition to measuring the average value of the shape statistic for the entire ensemble we also study the shape of an individual cluster by choosing a window large enough to enclose the entire cluster and by setting the density at all but points on the cluster to zero. The origin about which the moments of the density field are computed is the center of mass of the cluster.

In Fig. 2 we have shown the histogram of the three structure functions of isolated clusters, computed as described above, and plotted as a function of the cluster mass. In all the panels linearity is shown as a thick solid line, planarity as a dotted line and sphericity as a dashed line. The height of the histogram on a given mass scale represents the average value of the corresponding statistic obtained using an ensemble of four distinct realizations of a single power spectrum, error bars are 1σ dispersions over the ensemble. As in Fig. 1 left panels correspond to $n = -2$ models and right panels to $n = 0$ models, the scale of nonlinearity increases from top to bottom. In both spectra at earlier epochs the statistics suggests that clusters are predominantly spherical irrespective of their mass. With the onset of nonlinearity on larger scales, first low mass clusters begin to develop filamentarity and, at later epochs, larger clusters too become filamentary (this effect is particularly noticeable for $n = -2$). Except on the very largest scales (and during some epochs) filamentarity dominates over planarity, the difference between the two being statistically significant.

For the largest structures the measure of sphericity must be treated with some caution. In particular it is worth stressing that when measured on the largest scales, the statistics we use *cannot* distinguish between a web of connected filaments bordered by a large sphere from a smooth mass distribution in a similar sphere.

In Fig. 3 we plot structure functions averaged over many random but high density points as functions of the window size R. Curves are as in Fig. 2 except that here we show four epochs in the same panel with heavier lines representing later stages of nonlinearity. The average value of shape functions spectacularly demonstrates our claim concerning the emergence of filamentarity as gravitational clustering proceeds from the mildly to the strongly nonlinear regime. We see that structures tend to become oblate *only after* a filament-like shape has already developed. We find that (except on the largest scale) prolateness dominates over oblateness at all epochs for both spectra. It is likely that at later epochs neighboring clusters align themselves leading to the increasing amplitude of curves representing filamentarity in Fig. 3. This behavior is seen for planarity too although at a smaller amplitude.

We conclude our analysis of: (i) shapes of isolated clusters and (ii) shapes of overdense regions averaging all clusters, by emphasising that filamentarity dominates over planarity for both (i) and (ii), growing more pronounced at later epochs. Although almost always weaker

than filamentarity, planarity too is statistically significant. Thus, the mass distribution in a generic cosmological scenario of gravitational clustering is in a good *qualitative* agreement with the galaxy distribution characterized as "a network of surfaces" by de Lapparent et al (1991).

It is worth stressing that the visual dominance of filaments over planar structures in the density distribution is typical even for classical pancake models such as the HDM scenario (Klypin & Shandarin 1983). The underlying generic singularities (to be realized at later times) other than pancakes were suggested to explain qualitatively this phenomena (Arnol'd et al. 1982). Thus, the results of this paper do not contradict the conclusion that the first singualrities are pancakelike (Shandarin et al. 1995).

Since filamentarity increases with decreasing spectral index n, we expect to see more filamentary objects at higher redshifts in CDM-like models for which the effective index shows a significant tilt towards smaller scales.

Clearly an important issue not resolved in the present paper, concerns the *quantitative* morphology and shape analysis of three dimensional galaxy distributions. We shall address this issue in a subsequent paper (Sathyaprakash et al. 1995b), where we evaluate structure functions for the IRAS density map.

REFERENCES

Arnol'd, V.I., Shandarin, S.F., & Zel'dovich, Ya.B. 1982, Geophys. Astrophys. Fluid Dynamics, 20, 111

Babul A., & Starkman G.D. 1992, ApJ, 401, 28

Dominik K., & Shandarin S.F. 1992, ApJ, 393, 450

Klypin A.A., & Shandarin S.F. 1983, MNRAS, 204, 891

Klypin A.A., & Shandarin S.F. 1993, ApJ, 413, 48

de Lapparent, V., Geller, M.J., & Huchra, J.P. 1991, ApJ, 369, 273

Melott, A.L, & Shandarin, S.F. 1993, ApJ, 410, 469

Pearson R.C., & Coles P. 1995, MNRAS, 272, 231

Sahni V., & Coles P., 1995, Physics Reports, 262, 1

Sathyaprakash B.S., Sahni V., & Shandarin S.F. 1995a, MNRAS, submitted

Sathyaprakash B.S., Sahni V., Shandarin S.F., & Fisher K. 1995b, in preparation

Shandarin, S.F. 1983, Soviet Astron. Lett., 9, 104

Shandarin, S.F., & Zel'dovich Ya. B. 1983, Comments Astrophys., 10, 33

Shandarin, S.F., Melott, A.L., McDavitt, K., Pauls, J.L., & Tinker, J. 1995, Phys. Rev. Lett., 75, 7

Yess C., Shandarin S.F., 1996, ApJ, to be published
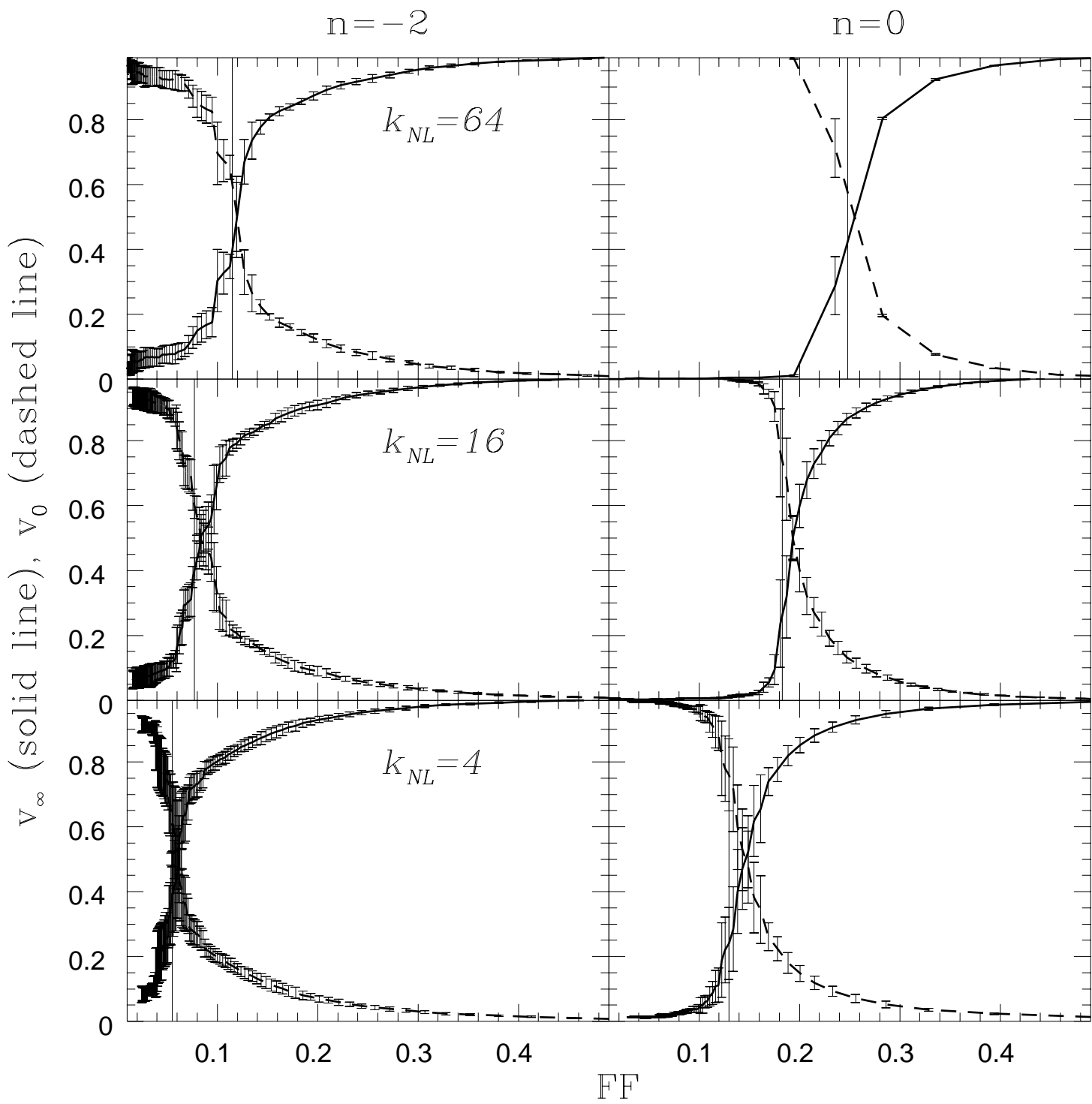
Zel'dovich Ya. B., 1982, Soviet Astron. Lett., 8, 102

Fig. 1.— Percolation transition in $n = -2$ model (left panels) and $n = 0$ model (right panels) at different epochs measured by the scale of nonlinearity k_{NL}^{-1} which increases from top to bottom. The filling factor of the largest cluster v_∞ (solid line) and the filling factor of all but the largest cluster v_0 (dashed line) (both measured in units of the total filling factor) are plotted against the total filling factor FF.

Fig. 2.— The average linearity (solid lines), planarity (dotted lines) and sphericity (dashed lines) of clusters belonging to a given mass range are plotted as functions of cluster mass. As in Fig. 1 the scale of nonlinearity increases from top to bottom.

Fig. 3.— Structure functions averaged over random (but high density) points are shown as functions of the window radius R (measured in units of the grid size). Curves are for the epochs $k_{\mathrm{NL}} = 32, 16, 8$ and 4 (in units of the fundamental mode) with heavier lines corresponding to later epochs.